Proton-exchange membrane (PEM) fuel cell system mathematical modelling

Abdelnasir Omran[1], David I. Smith[2], Abed Alaswad[3], Amirpiran P. Amiri[4], José R. Sodré[*5]
[1]School of Engineering and Applied Science
Aston University, Birmingham, UK
e–mail: [1]omrana@aston.ac.uk, [2]d.i.smith@aston.ac.uk, [3]a.alaswad@aston.ac.uk,
[4]a.p.amiri@aston.ac.uk, [5]j.sodre@aston.ac.uk

Alessandro Lucchesi
School of Engineering
University of Pisa, Pisa, Italy
e–mail: 180208173@aston.ac.uk

ABSTRACT

This work presents a mathematical modelling of a proton-exchange membrane (PEM) fuel cell system integrated with a resistive variable load. The model was implemented using *MATLAB Simulink* software based on an *H-500xp* pinch top PEM fuel cell type, and it is used to calculate the reference fuel cell current at various steady-state conditions. The reference current is the input value for the simulation of the PEM fuel cell performance. The model was validated using a *Horizon H-500xp* model fuel cell stack system, with the following components: a 500 W PEM fuel cell, a 13.5 DC volt battery for the start-up, a super-capacitor bank to supply peak loads and a 48 V DC-DC boost converter. In addition, the generated power is dissipated by a variable resistive load. The results from the model shows a qualitative agreement with test bench results, with similar trends for stack current and voltage in response to load and hydrogen flow rate variation. The discrepancies ranged from 5% to 10%, depending on the load resistance applied. Both model and experiments showed a hydrogen conversion efficiency of 80%.

KEYWORDS

Fuel cell, hydrogen, mathematical model, energy conversion management, performance, bench testing.

INTRODUCTION

The increase in greenhouse gases (GHGs) has joined industries and governments to find solutions to reduce GHGs, especially from the transportation sector. A recent study [1] reports the past two hundred years have shown a 30% increase in atmospheric carbon dioxide (CO_2) and an average temperature rise of 0.6°C on the planet. Many efforts using biofuels, especially biodiesel and alcohol blends with conventional fuels, were used [2, 3] as alternatives to solve the problem. Recent progress in fuel cell technology and electric cars can revolutionise the future scenario of transportation vehicles [4, 5]. Although there are many types of fuel cells, the proton exchange membrane fuel cell (PEMFC) type has captured more attention for vehicular application. Fuel cells are energy conversion devices that convert the chemical energy of hydrogen into electrical energy. The conversion requires a battery for a start-up, air and fuel

[*] Corresponding author

supply, heat removal, and exhaust. The main difference from conventional internal combustion engines (ICE) is that fuel cells are zero-emission devices which exhaust is primarily water vapour [6]. Both fuel cells and batteries promote electrochemical conversion and are normally arranged into stacks. However, unlike batteries, fuel cells do not require recharging and can continuously operate fed with hydrogen and oxygen or air. On the other hand, fuel cells have a broader group of ancillaries, and controlling them during operation is a difficult task as they affect performance and efficiency. Scaling up the stacks do not require a significant effort, but the difficulty is upgrading the ancillaries, which entails complete change.

The complexity of fuel cell systems makes mathematical modelling a convenient research strategy to save time, reduce cost and provide in-depth analysis of various parameters that affect fuel cell performance and efficiency such as stack temperature, pressure, reactant moisture and air stoichiometry. A previous study using a one-dimensional mathematical model for a fully hydrated and isothermal PEMFC concluded that the higher the cell current density, the greater the threshold of oxygen or air bleeding [7]. Simulink modelling was successfully used to control the temperature of a PEMFC stack and keep it in a small range near the target value [8].

A recent study on various DC-DC converter topologies to form a segment of bus microgrid concluded that unidirectional and bidirectional isolated current-fed DC-DC converters are preferred for fuel cells and ultracapacitors, respectively [9]. A bench test study using a mathematical model to simulate the ability of a battery-PEMFC hybrid control system proved its efficiency to manage the energy of an electric vehicle [10]. A research on PEMFC energy management control for hybrid vehicle [11] has advocated the use of mathematical modelling to reduce cost and time of investigation activity. Modelling has been used across all types of fuel cells such as solid oxide fuel cell [12 - 16].

This work aims to develop a mathematical steady-state modelling of a PEMFC system using MATLAB Simulink and compare it results with experiments in a test bench. The mathematical model simulates the output current, voltage and power of the fuel cell, analysing the response of the system with different external loads. The model is compared using the commercial Horizon H-500XP fuel cell stack, which main components are a 500W PEMFC stack, a 12 VDC battery for the start-up and a bank of super-capacitors to supply additional power. In addition to that, the generated power is dissipated in a variable resistive load, where the voltage is maintained constant by a 48-volt DC-DC boost converter.

EXPERIMENTAL SETUP

Fuel cell system

The H-500XP model PEM fuel cell stack used in this work has 30 cells with a peak power of 600W [17]. The current varies from 0 A to 33.5A, and DC voltage ranges from 15 V to 28.8 V. The rated current is 33.5 A at 18 V. The stack is self-humidified, and is operated with high purity hydrogen (99.99 % dry H_2) and air for the reaction. Cooling is provided by two axial fans. Figure 1 shows all the fuel cell system components, with the boost converter and the external load. Other than the stack, the main components of the H-500XP system are the fuel supply, purging valves and pipe, battery, super-capacitor bank, and system controller.

The fuel cell battery operates for the start-up, and the super-capacitor operates supplying power during short circuit or when the stack output power demanded is over 500 W [17]. The controlled system parameters are stack temperature, through variation of the fan velocity, fuel purging valve opening, and fuel supply. The controller also monitors the stack voltage, current and temperature, preventing over-current, low-voltage and high temperature.

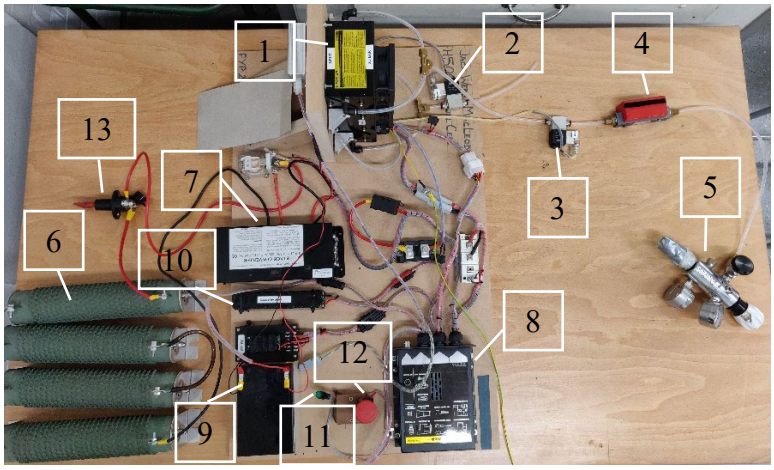

1	PEMFC stack
2	Purging valve
3	Supply valve
4	Fuel flowrate sensor
5	Hydrogen cylinder regulator
6	Load bank resistors
7	DC-DC converter
8	System controller
9	Battery
10	Ultra-capacitor
11	On-off switch
12	Emergency stop switch
13	Load bank circuit breaker

Figure 1. H-500XP and auxiliaries

The H-500XP stack system is connected to a hydrogen cylinder, a DC boost converter, and external resistive loads, which provide variable power demand. The boost converter ensures 48 V voltage across the load system. The power is dissipated to the resistance as heat by the Joule effect. Figure 2 shows the PEMFC system (1) in a purpose built casing, bank of electric resistances (2), and load controller (3).

Figure 2. PEMFC test set

Test procedure

The pressure regulator attached to the hydrogen cylinder connected to the PEMFC system was set to supply 1.5 bar absolute. The PEMFC system was monitored using a dedicated software provided by the manufacturer. The battery was used for start-up and then disconnected. The load variation were applied through the load bank control keys. The system was tested increasing the load, starting from open-circuit condition and gradually reducing to the lowest external load resistance of 4.63 Ω. For every load change, 1 min was allowed to reach the steady-state condition before making the measurement readings. Then, the readings were recorded along 5 min at a given load. Hydrogen flow rate was recorded by a digital flowmeter

positioned between the cylinder and the stack inlet. The instantly acquired data to be processed by the software were: stack voltage (V), stack current (I), stack output power (W), stack temperature (°C), ambient temperature (°C), and battery voltage (V).

MATHEMATICAL MODELLING

Fuel cell stack model

Fuel cells are commonly modelled with mathematical equations where the current is an independent variable and is used to calculate the stack voltage. In the presented model, the external load resistance is the independent parameter to influence current and voltage [18]. The fuel cell stack has been modelled with a DC voltage source controlled by equations that relate fuel cell stack current and temperature with its voltage. The stack current flows from the voltage source to the circuit. The voltage source supplies energy to an electrical circuit made by a DC boost converter and variable load. The converter is controlled by a voltage Proportional-Integral (PI) controller with pulse-width modulation (PWM) signal control. The controlled current source models the power consumption of auxiliary components. The whole model is developed with MATLAB Simulink, including its package Simscape to solve the electrical circuit.
The stack was modelled as one-dimensional and isothermal, and steady state operating conditions were assumed. The partial pressure of the reactants was taken as constant, the rise of pressure due to the blower and pressure drop of the fuel flow in the pipe was neglected. The humidity of the membrane was considered constant at saturated conditions. Power consumption of the auxiliary components was also taken as constant. As the transient conditions during start-up is not taken in account by the model, the battery and super-capacitor are not included. The maximum power demand was considered as 500 W.

Hydrogen (H_2) reaction with oxygen (O_2) in a single cell with liquid water (H_2O) as product is written as:

$$H_2 + \frac{1}{2} O_2 \rightarrow H_2O \tag{1}$$

Based on Eq. (1), the reversible open-circuit voltage at the reference condition (298.15 K, 1 bar), E^0, is given by [19]:

$$E^0 = \frac{-\Delta g_f}{2F} = 1.229\ V \tag{2}$$

Where Δg_f (k*J/kmol*) is the variation in the Gibbs free energy of formation and F is the Faraday constant ($96485\ C$).
Using Nernst's equation, the reversible open-circuit voltage, $E^{T,P}$ (V), can be evaluated at different conditions [2]:

$$E^{T,P} = \frac{-\Delta g_f}{2F} + \frac{RT_s}{2F} ln\left(\frac{p_{H_2} \cdot {p_{O_2}}^{\frac{1}{2}}}{p_{H_2O}}\right) - \frac{\Delta S}{2F}(T_s - 298.15) \tag{3}$$

Where T_s is the stack temperature (K), R is the universal gas constant (8.314 kJ/kmol.K), p is the partial pressure of reactants and products (bar), and ΔS is the entropy variation (kJ/kmol.K). When load is applied, the external current I_{ext} (A) flows and the voltage drops. During operation, a small amount of hydrogen can diffuse through the membrane from the anode to the cathode, where it reacts without producing current and some electrons may cross through the

membranes rather than the external load. Those effects are equivalent and are considered by adding a current loss, I_{loss} (A) to the total fuel cell current I (A), as shown by:

$$I = I_{ext} + I_{loss} \tag{4}$$

where only I_{ext} can be collected by the external load [19].
The voltage needed to keep the electrochemical reactions in the anode and cathode represents the activation voltage losses, ΔV_{act} (V), which can be calculated as [20]:

$$\Delta V_{act} = \xi_1 + \xi_2 T_s + \xi_3 T_s \, ln(C_{O_2}) + \xi_4 T_s \, ln(I) \tag{5}$$

Where the constant parameters $\xi_1 \ldots \xi_4$ are shown by Tab. 1, and C_{O_2} is the concentration of dissolved oxygen (mol/cm^3) at the liquid interface as defined by Henry's law [21]:

$$C_{O_2} = \frac{p_{O_2}}{5.08 \cdot 10^6 exp\left(-\frac{498}{T_s}\right)} \tag{6}$$

The ohmic voltage losses, ΔV_{ohm} (V), are described by [19]:

$$\Delta V_{ohm} = R_{ion} I + (R_{ele} + R_{con}) I_{ext} \tag{7}$$

Where R_{ion} (Ω) is the resistance to the flow of ions in the membrane, R_{ele} (Ω) is the electronic resistance to the flow of electrons in the conductive material, and R_{con} (Ω) is the contact resistance of the electrodes. Only R_{ion} is considered and, for a Nafion membrane, it is given by [22]:

$$R_{ion} = \frac{r_{ion}}{A} = \frac{1}{A} \cdot \frac{\tau_m}{\sigma_m} = \frac{1}{A} \cdot \frac{\tau_m}{(0.005139\lambda_m - 0.00326) \cdot exp\left[1268\left(\frac{1}{303} - \frac{1}{T_s}\right)\right]} \tag{8}$$

Where τ_m is the membrane thickness (cm^2), σ_m is the ionic conductivity of the membrane (Ω/cm), and A is the single cell active area (cm^2). λ_m is the average water content of the membrane and is a function of the water activity a, both dimensionless [23]:

$$\lambda_m = \begin{cases} 0.043 + 17.81a - 39.85a^2 + 36.0a^3 & for \ 0 < a \leq 1 \\ 14 + 1.4(a-1) & for \ 1 < a \leq 3 \end{cases} \tag{1}$$

Concentration voltage losses (ΔV_{con}) occur at the high current caused by reduction in gas concentration at the electrode surface, and are given by [19]:

$$\Delta V_{con} = \frac{RT}{n_c F} ln\left[0.21\left(\frac{I_{L,c}}{I_{L,c} - I}\right)\right] + \frac{RT}{n_a F} ln\left(\frac{I_{L,a}}{I_{L,a} - I}\right) \tag{10}$$

Where I_L (A) is the limit current of the electrode, which occurs when the partial pressure of the reactants falls down to zero; n_a and n_c are the number of electrons involved in the anode and cathode reactions, respectively. Anode concentration losses are considered negligible.
The polarisation curve of the fuel cell stack is then described by:

$$V_{stack}(I) = n_{cell}V_{cell}(I) = n_{cell}(E - \Delta V_{act} - \Delta V_{ohm} - \Delta V_{con})$$
$$= n_{cell}\left\{E - \left[\xi_1 + \xi_2 T_s + \xi_3 T_s\, ln(C_{O_2}) + \xi_4 T_s\, ln(I)\right] - R_{ion}I\right.$$
$$\left. - \frac{RT}{n_c F} ln\left[0.21\left(\frac{I_{L,c}}{I_{L,c} - I}\right)\right]\right\} \quad (11)$$

Where the number of cells connected in series, n_{cell}, is 30.
The output power of the stack is given by:

$$P_{stack} = V_{stack}I_{ext} \quad (12)$$

Table 1 shows all the PEMFC model parameters.

Table 1. PEMFC model parameters

PARAMETER	VALUE	PARAMETER	VALUE	PARAMETER	VALUE
$p_{H_2}\ (bar)$	1.5	ξ_1	1.01	$\tau_m\ (cm)$	150×10^{-4}
$p_{O_2}\ (bar)$	0.21	ξ_2	-3.54×10^{-3}	λ_m	14
$p_{H_2O}\ (bar)$	1	ξ_3	-7.80×10^{-5}	$A\ (cm^2)$	50
$I_{loss}\ (A)$	0.3	ξ_4	1.96×10^{-4}	$I_{L,c}\ (A)$	80

Boost converter and external load model

The use of a PEM fuel cell in a hybrid system requires a DC converter, mostly boost converter. A basic DC boost converter scheme is presented in Figure 3 [24].

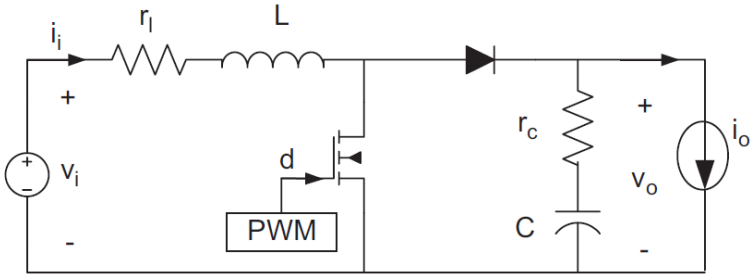

Figure 3. DC boost converter circuit [24]

The PWM signal commands the opening and the closing of a switcher with a fixed switching frequency $F_{SW}\ (Hz)$. The corresponding period of switching is the sum of ON and OFF times [25]:

$$T_{SW} = \frac{1}{F_{SW}} = T_{ON} + T_{OFF} \quad (13)$$

The duty cycle is defined as the portion of time when the switcher is 'ON state', as [25]:

$$d = \frac{T_{ON}}{T_{ON} + T_{OFF}} \quad (14)$$

Assuming the switcher, the diode, the inductor (L) and the capacitor (C) are ideal, the equations that relate the duty cycle (d), the converter input voltage (V_I) and current (I_I) and the output voltage (V_O) and current (I_O) are given by [24]:

$$\frac{V_O}{V_I} = \frac{1}{1-d} \tag{15}$$

$$\frac{I_O}{I_I} = 1-d \tag{16}$$

Applying Ohm's law on the external load resistance (R_{load}), one can obtain [24]:

$$R_{load} = \frac{V_O}{I_O} = \frac{\frac{V_I}{(1-d)}}{I_I(1-d)} \tag{17}$$

The equivalent resistance to the fuel cell is given by [24]:

$$R_{eq} = \frac{V_I}{I_I} = R_{load}(1-d)^2 \tag{18}$$

Equation (18) shows the effect of the duty cycle on the fuel cell operating point, the highest value of duty cycle leads to the lowest equivalent resistances sensed by the fuel cell and, therefore, to the highest current and power demand. The PI controller controls the value of the duty cycle, ensuring 48 V for every external load.

The size of the reactive elements of the boost converter is chosen to limit the input current ripple (fuel cell current ripple) and the output voltage ripple as well. Limiting the fuel cell current ripple is necessary to ensure a longer lifetime of the fuel cell. In a fuel cell sudden changes in current should be limited as well to avoid starvation problems and degradation of a catalyst layer. This is typically done by controlling the fuel cell current with the boost converter [26]. In this model, however, the controller of the boost converter is a simple PI voltage controller that guarantees an output voltage of 48 volts, but it does not take into account the fuel cell current variation. The maximum current and voltage ripple allowed and the parameters used for the DC boost converter and the PI controller are shown in Table 2.

Table 2. DC boost converter and PI controller parameters

DC BOOST CONVERTER	VALUE	PI CONTROLLER	VALUE
Switching frequency (kHz)	50	k_P	0.004
Maximum input current ripple (%)	4	k_I	1.15
Maximum output voltage ripple (%)	2	Duty cycle range	$0.1 - 0.7$
Inductance (mH)	1.85		
Capacitance (μF)	500		

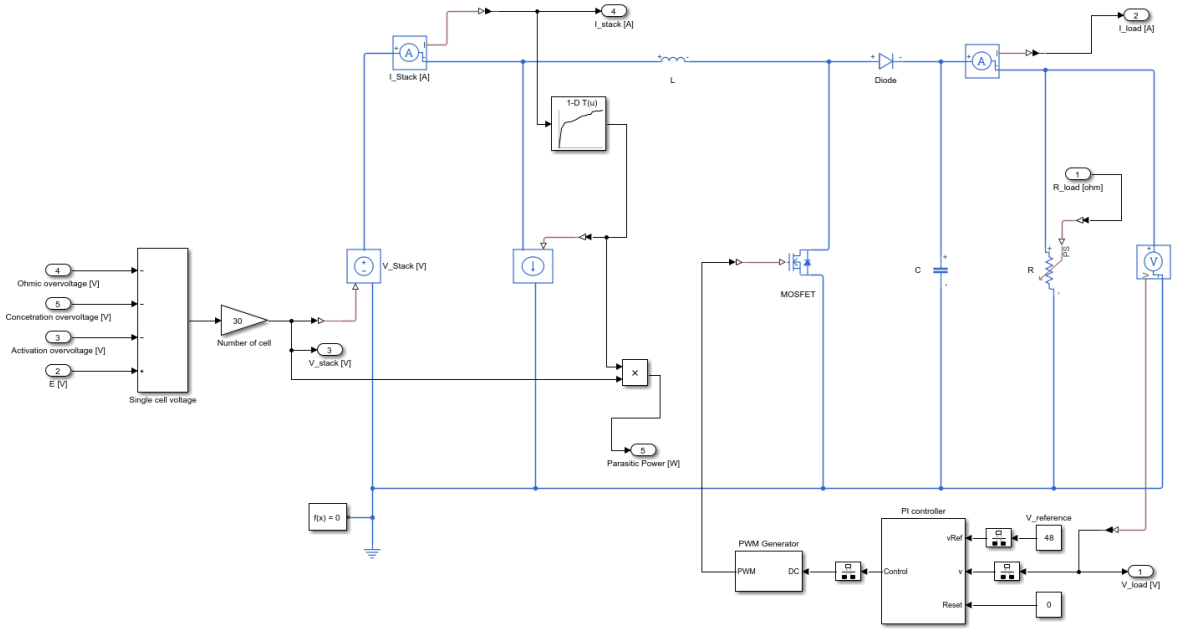

Figure 4. PEMFC system equivalent electrical circuit

Figure 4 shows the PEMFC equivalent electrical circuit. The fuel cell is modelled with a controlled DC voltage source $V_{stack}(I)$ which is connected to an electric circuit. The value of output current of the stack is taken from the circuit and is used to update the value of the output voltage of the stack. The fuel cell stack is connected to a DC boost converter, which enhances the output voltage of the stack to 48 V at the resistance load bank. A PWM signal, controlled by a PI controller, is used to adjust the duty cycle of the boost converter. After the stack, a controlled current source is used to simulate the power consumption of the auxiliary components, considered constant with stack current and temperature at 40 W $\pm$ 1 W.

Performance parameters calculation

For a specific external load resistance (R_{load}), the theoretical power request (P_{req}) from the stack is calculated by

$$P_{req} = \frac{48^2}{R_{load}} \tag{19}$$

The efficiency of the boost converter (η_{con}) is given by its output power divided by its input power. Therefore dividing the power delivered to the load (P_{load}) by the output power of the stack minus power consumption by auxiliary components, the efficiency of the boost converter can be calculated as:

$$\eta_{con} = \frac{P_{out}}{P_{in}} = \frac{P_{load}}{P_{stack} - P_{auxiliaries}} = \frac{\frac{V_{load}^2}{R_{load}}}{V_{stack} I_{ext} - P_{auxiliaries}} \tag{20}$$

Where V_{load} is the voltage across the external load (48 V).
The stack efficiency is calculated by:

$$\eta_{stack} = \frac{P_{stack} - P_{auxiliaries}}{P_{fuel}} = \frac{V_{stack} I_{ext} - P_{auxiliaires}}{\dot{V}_{fuel} \cdot \rho_{fuel} \cdot LHV_{H_2}} \tag{21}$$

Where P_{fuel} is the power input of hydrogen (W) which is given by the product of its flow rate $\dot{V}_{fuel}$ (m^3/s) multiplied by its density ρ_{fuel} (kg/m^3) and lower heating value LHV_{H_2} (kJ/kg). The number of moles of hydrogen consumed by the stack for the reactions and for losses due to internal fuel crossover, $\dot{N}_{H_2}$ (mol/s), is obtained by [27]:

$$\dot{N}_{H_2} = \dot{N}_{fuel} = \frac{n_{cells} I}{2F} \tag{22}$$

Which is essentially equal to the moles of fuel because hydrogen with a purity degree of 99.99% has been used. Assuming that the fuel utilisation factor is $\eta_{fu} = 80\ \%$ and that hydrogen behaves as an ideal gas then, the actual fuel volumetric flow rate, $\dot{V}_{fuel}$ (m^3/s), is calculated as:

$$\dot{V}_{fuel} = \dot{N}_{fuel} \cdot \tilde{v}_{fuel} \cdot \frac{1}{\eta_{fu}} = \dot{N}_{fuel} \frac{RT_{fuel}}{p_{H_2}} \cdot \frac{1}{\eta_{fu}} \tag{23}$$

Where T_{fuel} is the fuel temperature set to the room temperature at $293.15\ K$.
The global efficiency of the system is given by the product of the efficiency of the DC boost converter and the efficiency of the stack, which becomes:

$$\eta_{syst} = \eta_{stack}\eta_{con} = \frac{P_{load}}{P_{fuel}} = \frac{\frac{V_{load}{}^2}{R_{load}}}{\dot{V}_{fuel} \cdot \rho_{fuel} \cdot LHV_{H_2}} \tag{24}$$

RESULTS AND DISCUSSION

Figure 5 shows the fuel cell stack polarisation curve, which represents the steady state operating states. The experimental values were fairly close to the model polarisation curve, thus validating the model built for the PEMFC stack. As the manufacturer rated fuel cell power of 500W, the lowest external load resistance tested was 5.47 Ω, corresponding to the maximum electric current of 25 A.

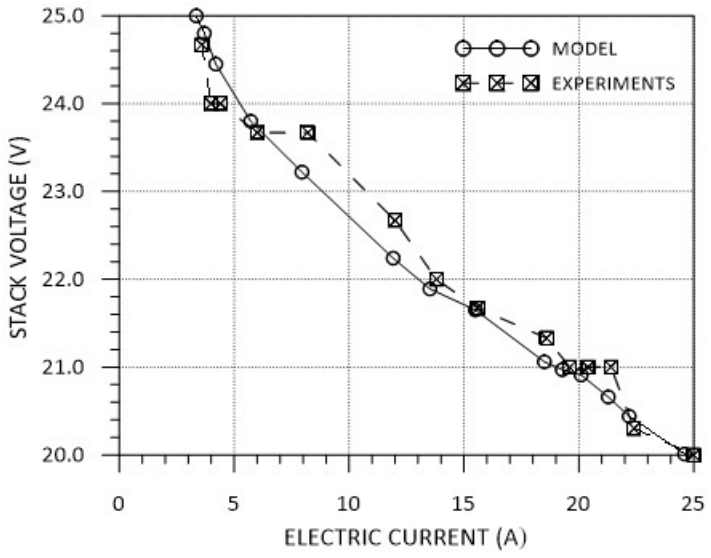

Figure 5. Polarisation curve of the PEMFC stack model

In Fig. 6, the steady-state values of current with different external load resistance is shown for the model and the experimental data. Lower external load resistance means higher power demand from the PEMFC stack, therefore higher current. According to the dependence of the output voltage of the stack with its current (Fig. 7), with an increase of external load resistance lower current occurs and, therefore, higher stack output voltage values have been observed in the experiments and agreed by the model.

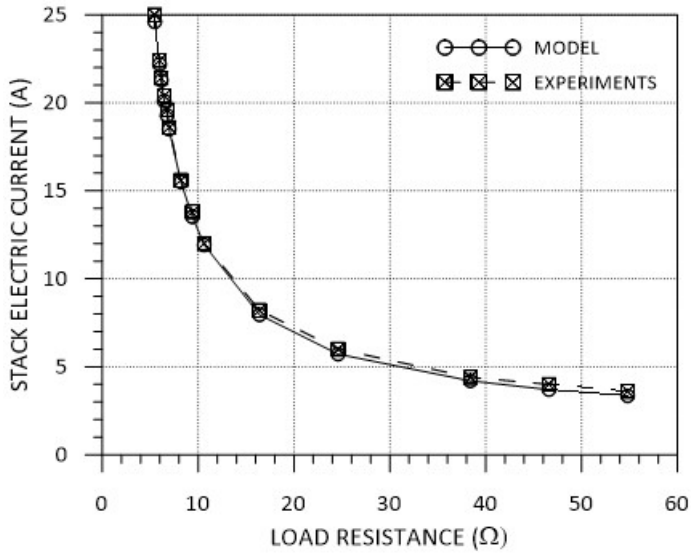

Figure 6. Stack current variation with external load resistance

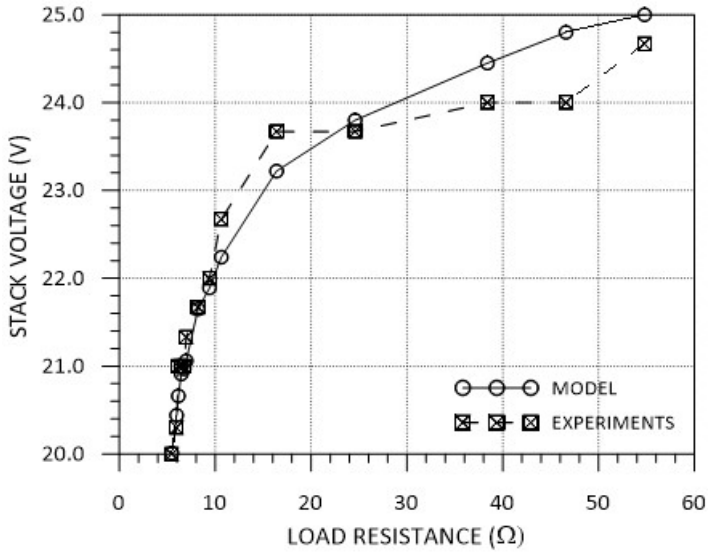

Figure 7. Stack voltage variation with external load resistance

In Figure 8 it is noticed the increase of the stack output power with the decrease of the external load resistance. Fuel cell power output is incremental with the current; therefore when a decrease in the external load resistance occurs, the stack will raise its output current and consequently be fed with higher fuel flow rate by the controller.
As shown in Fig. 9, with the assumption of hydrogen utilisation of 80%, the fuel flow rates predicted by the model match the experimental values. Therefore, the assumption is considered reasonable, even if a discrepancy can be observed above 200 W.

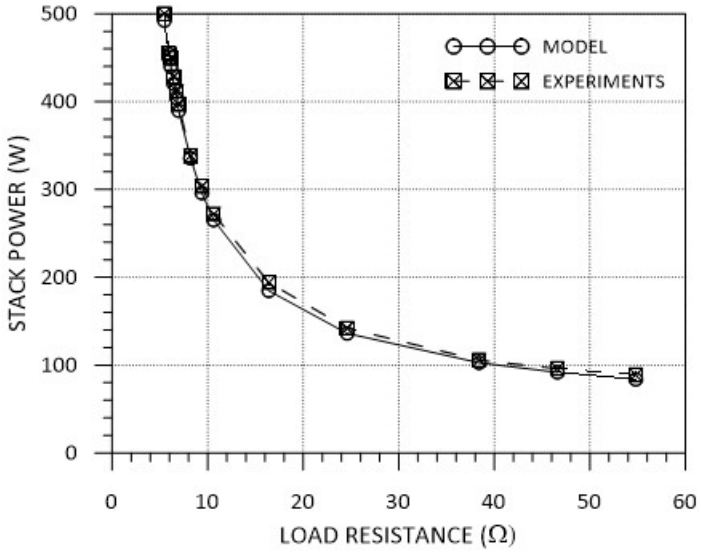

Figure 8. Output stack power variation with external load resistance

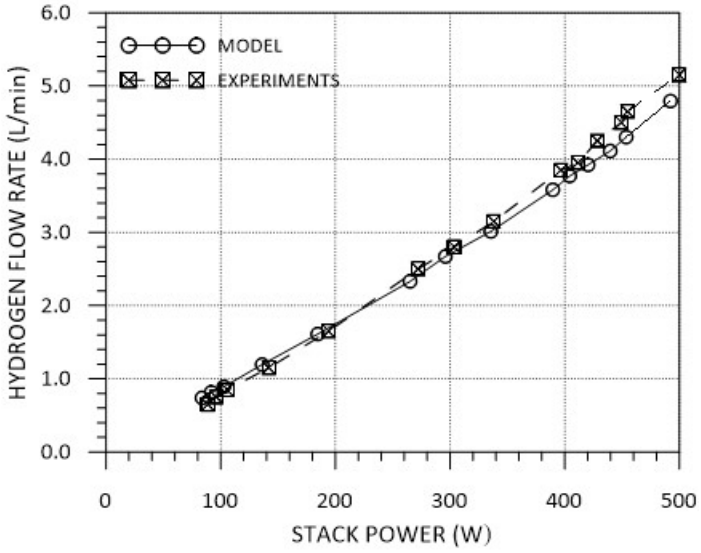

Figure 9. Fuel flow rate variation with different output stack power

Figure 10 shows the global system efficiency for model and experiments. For output stack power above 200W the efficiency predicted by the model is overestimated, mainly caused by the assumption of 80% fuel utilisation while in the experiments it fluctuated between 74% and 90%, with lower values for higher output stack power. For every value of external load tested the efficiency of the DC boost convert was in the range of 92-97% for both model and experimental results.

The fuel supply tubes from the cylinder to the fuel cell presented no leakage, as the hydrogen sensor indicated. The internal fuel crossover cannot explain such low values of hydrogen utilisation (Fig. 10). Higher flow rates from the cylinder generally mean lower fuel temperatures (Joule Thomson effect as gas expands from 150 bar to 0.5 bar), which could lead to an overestimation of volume flow rate at higher loads. During operation, some hydrogen was purged through the purging valve, which may have contributed to the loss of efficiency. The purging system, precise measurement of hydrogen temperature, and hydrogen consumption using other measurement methods are subjects of future investigation.

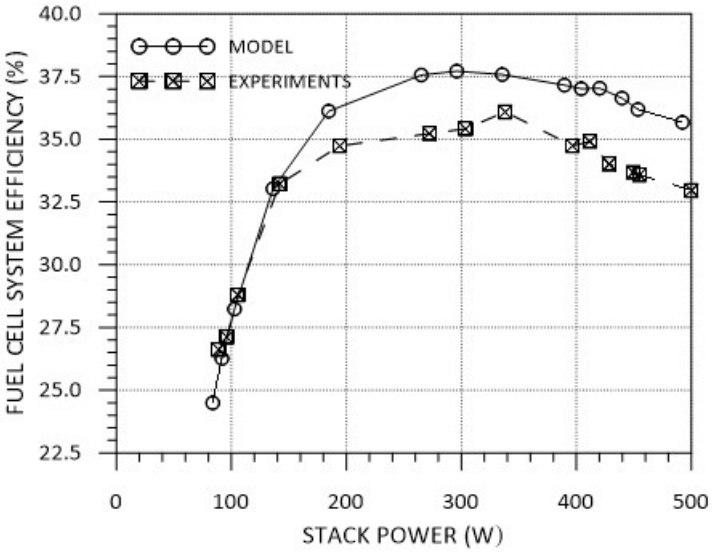

Figure 10. Global system efficiency with different output stack power

CONCLUSION

A steady-state model that simulates the output current and voltage of a PEM fuel cell stack with varying external load was presented and validated by experiments in a test bench. By decreasing the load resistance the stack current kept increasing, the maximum current being achieved with the lowest external load resistance. With a load resistance of 54.80 Ω, the stack current was almost 3.60 A, which was 10% higher than the model calculation. With a load resistance of 16.40 Ω the stack current reached 8.20 A, with a discrepancy less than 5% to the model. At 5.47 Ω the measured current was 25 A, less than 2% higher than the model value. Consequently, with the increase of the stack current the stack voltage decreased from 24.67 V (at 54.80 Ω) to 20.00 V (at 5.47 Ω). The fuel flow rate calculated by the model, with an assumption of fuel utilisation equal to 80%, was close to the measured fuel flow rate. The difference in fuel flow rate seen for stack output power higher than 200W is the leading cause of the discrepancy in system efficiency, which nevertheless was kept below 3%.

ACKNOWLEDGMENT

The authors thank the School of Engineering and Applied Science at Aston University and the University of Pisa for their support to this project.

REFERENCES

1. K. Haraldsson, “On Direct Hydrogen Fuel Cell Vehicles-Modelling and Demonstration.”
2. O. S. Valente, V. M. D. Pasa, C. R. P. Belchior, and J. R. Sodré, “Physical–chemical properties of waste cooking oil biodiesel and castor oil biodiesel blends,” 2011.
3. A. K. K. Hossain *et al.*, “Combustion of fuel blends containing digestate pyrolysis oil in a multi-cylinder compression ignition engine,” *Fuel*, vol. 171, pp. 18–28, May 2016.
4. F. Stodolsky, F. An, L. Gaines, C. L. Marshall, and J. J. Eberhardt, “Total Fuel Cycle Impacts of Advanced Vehicles,” *SAE Tech. Pap. Ser.*, vol. 1, no. 724, 2010.
5. A. Alaswad, A. Baroutaji, H. Achour, J. Carton, A. Al Makky, and A. G. Olabi, “Developments in fuel cell technologies in the transport sector,” *Int. J. Hydrogen Energy*, vol. 41, no. 37, pp. 16499–16508, 2016.
6. D. H. Swan, B. E. Dickinson, and M. P. Arikara, “Proton Exchange Membrane Fuel Cell Characterization for Electric Vehicle Applications,” *SAE Tech. Pap. Ser.*, vol. 1, no. 412, 2010.
7. J. J. Baschuk and X. Li, “Mathematical model of a PEM fuel cell incorporating CO poisoning and

O<SUB align=right>2 (air) bleeding," *Int. J. Glob. Energy Issues*, vol. 20, no. 3, p. 245, 2003.
8. S. Cheng, C. Fang, L. Xu, J. Li, and M. Ouyang, "Model-based temperature regulation of a PEM fuel cell system on a city bus," *Int. J. Hydrogen Energy*, vol. 40, no. 39, pp. 13566–13575, Oct. 2015.
9. O. A. A. Ahmed and J. A. . A. M. Bleijs, "An overview of DC–DC converter topologies for fuel cell-ultracapacitor hybrid distribution system," *Renew. Sustain. Energy Rev.*, vol. 42, pp. 609–626, Feb. 2015.
10. Z. Mokrani, D. Rekioua, N. Mebarki, T. Rekioua, and S. Bacha, "Proposed energy management strategy in electric vehicle for recovering power excess produced by fuel cells," *Int. J. Hydrogen Energy*, vol. 42, no. 30, pp. 19556–19575, 2017.
11. P. M. Muñoz, G. Correa, M. E. Gaudiano, and D. Fernández, "Energy management control design for fuel cell hybrid electric vehicles using neural networks," *Int. J. Hydrogen Energy*, vol. 42, no. 48, pp. 28932–28944, 2017.
12. A. Amiri *et al.*, "Planar SOFC system modelling and simulation including a 3D stack module," *Int. J. Hydrogen Energy*, vol. 41, no. 4, pp. 2919–2930, 2016.
13. S. Tang, A. Amiri, and M. O. Tadé, "System Level Exergy Assessment of Strategies Deployed for Solid Oxide Fuel Cell Stack Temperature Regulation and Thermal Gradient Reduction," *Ind. Eng. Chem. Res.*, p. acs.iecr.8b04142, 2019.
14. A. Amiri, S. Tang, P. Vijay, and M. O. Tadé, "Planar solid oxide fuel cell modeling and optimization targeting the stack's temperature gradient minimization," *Ind. Eng. Chem. Res.*, vol. 55, no. 27, pp. 7446–7455, 2016.
15. A. Amiri, K. Ahmed, and O. Tadé, "A steady-state and dynamic simulation tool for solid oxide fuel cell operation applications," pp. 1–6, 2019.
16. A. Amiri *et al.*, "Solid oxide fuel cell reactor analysis and optimisation through a novel multi-scale modelling strategy," *Comput. Chem. Eng.*, vol. 78, pp. 10–23, 2015.
17. H. F. C. System, "user manual," in *SpringerReference*, Berlin/Heidelberg: Springer-Verlag, 2011, pp. 1–53.
18. J. B. Benziger, M. B. Satterfield, W. H. J. Hogarth, J. P. Nehlsen, and I. G. Kevrekidis, "The power performance curve for engineering analysis of fuel cells," *J. Power Sources*, vol. 155, no. 2, pp. 272–285, 2006.
19. F. Barbir, *PEM fuel cells : theory and practice*. Academic Press, 2013.
20. M. A. I. Hooper, R. F. Mann, P. R. Roberge, J. C. Amphlett, H. M. Jensen, and B. A. Peppley, "Development and application of a generalised steady-state electrochemical model for a PEM fuel cell," *J. Power Sources*, vol. 86, no. 1–2, pp. 173–180, 2002.
21. P. R. Pathapati, X. Xue, and J. Tang, "A new dynamic model for predicting transient phenomena in a PEM fuel cell system," *Renew. Energy*, vol. 30, no. 1, pp. 1–22, 2005.
22. R. O'hayre, S. Cha, W. Colella, and F. Prinz, *Fuel cell fundamentals*, Third Edit. New Jersey: John Wiley & Sons, Inc, 2009.
23. I. M. M. Saleh, R. Ali, and H. Zhang, "Simplified mathematical model of proton exchange membrane fuel cell based on horizon fuel cell stack," *J. Mod. Power Syst. Clean Energy*, vol. 4, no. 4, pp. 668–679, 2016.
24. J. M. Andújar, F. Segura, and M. J. Vasallo, "A suitable model plant for control of the set fuel cell−DC/DC converter," *Renew. Energy*, vol. 33, no. 4, pp. 813–826, Apr. 2008.
25. E. Rogers, "Understanding Boost Power Stages in Switchmode Power Supplies Application Report," no. March, p. 36, 1999.
26. T. Pavlovic, T. Bjazic, and Z. Ban, "Modeling and current control of fuel cell-battery hybrid system with boost converter and input-output filters," *15th Int. Power Electron. Motion Control Conf. Expo. EPE-PEMC 2012 ECCE Eur.*, pp. 1–6, 2012.
27. F. Barbir, *PEM Fuel Cells: Theory and Practice*, Second Edi. Elsevier, 2013.